Discrepant gene functional potential and cross-feedings of anammox bacteria *Ca. Jettenia caeni* and *Ca. Brocadia sinica* in response to acetate

Ying Feng [a, b, 1], Yunpeng Zhao [a, b, 1], Bo Jiang [a, b], Huazhang Zhao [a, b], Qilin Wang [c], Sitong Liu [a, b, *]

[a] Department of Environmental Engineering, Peking University, Beijing 100871, China

[b] Key Laboratory of Water and Sediment Sciences, Ministry of Education of China, Beijing 100871, China

[c] Centre for Technology in Water and Wastewater, School of Civil and Environmental Engineering, University of Technology Sydney, Ultimo, NSW 2007, Australia

*** Corresponding author:** Sitong Liu

Address: College of Environmental Science and Engineering, Peking University, Yiheyuan Road, No.5, Haidian District, Beijing 100871, China.

E-mail: liusitong@pku.edu.cn

Tel/Fax: 0086-10-62754290.

[1] These authors contributed equally to this work.

Abstract: Although the enhancement of anammox performance for wastewater treatment due to the addition of small amount of acetate has been reported, discrepant metabolic responses of different anammox species have not been experimentally evaluated. Based on metagenomics and metatranscriptomic data, we investigated the competitiveness between two typical anammox species, *Candidatus Jettenia caeni* (*J. caeni*) and *Candidatus Brocadia sinica* (*B. sinica*), in anammox consortia under mixotrophic condition, where complex metabolic interactions among anammox bacteria and heterotrophs also changed with acetate addition. Contrary to *J. caeni*, the dissimilatory nitrate reduction to ammonium pathway of *B. sinica* was markedly stimulated for improving nitrogen removal. More acetate metabolic pathways and up-regulated AMP-*acs* expression for acetyl-CoA synthesis in *B. sinica* contributed to its superiority in acetate utilization. Interestingly, cross-feedings, including the nitrogen cycle, amino acid cross-feeding and B-vitamin metabolic exchange between *B. sinica* and other heterotrophs seemed to be enhanced with acetate addition, contributing to a reduction in metabolic energy cost to the whole community. Our work not only clarified the mechanism underlying discrepant responses of different anammox species to acetate, but also suggests a possible strategy for obtaining higher nitrogen removal rates in wastewater treatment under low C/N ratio.

Keywords: Anammox; Acetate; Cross-feedings; Metagenomics; Metatranscriptomics

1. Introduction

Depending on nutritional conditions, microorganisms may grow autotrophically, heterotrophically or mixotrophically (Smith et al., 1980). The growth rate and activity, as well as metabolic function, of microorganisms may vary with nutrient conditions. Generally, heterotrophs and mixotrophs grow at higher rates than autotrophs, as they are able to obtain more energy from organic substrates due to differences in metabolism (Kim et al., 2013). More importantly, intracellular metabolic pathways, as well as activities and gene functional potential, could be dissimilar even among different species within the same genus. Analysis based on comparative genomics have indicated that closely related strains may exhibit metabolic divergence due to genomic discrepancies (Bombar et al., 2014).

Wastewater is a complex mixture consisting of a wide range of organic matter, which inevitably affects the metabolic state of microorganisms in sludge during the treatment process (Le and Stuckey, 2016). Anaerobic ammonia oxidation (anammox), which is regarded as an energy-efficient process for wastewater treatment, has drawn a lot of attention recently (Kartal et al., 2010). Anammox bacteria are able to use, not only inorganic carbon sources, but also organic matter such as acetate and propionate for reducing inorganic nitrates/nitrate ions (NO_3^-) to ammonium cations (NH_4^+) via the dissimilatory nitrate reduction to ammonium (DNRA) pathway (Guven et al., 2005; Kartal et al., 2007a, 2007b; Van De Vossenberg et al., 2008). According to previous studies, organics may have an effect on the performance of the anammox

61 reactor (Tang et al., 2014) as well as on the functional gene expression profile (Shu et
62 al., 2015) and the microbial community structure (Leal et al., 2016). Responses of
63 different anammox species to organics seem to be distinct. For example, it was
64 reported that *Candidatus Jettenia asiatica (J. aiatica)* showed no superiority in
65 growth under mixotrophic conditions compared to autotrophs (Huang et al., 2014),
66 while other study found that the biomass of *Candidatus Brocadia fulgida (B. fulgida)*
67 showed an increase under certain C/N ratios (Jenni et al., 2014). However, the process
68 by which, organics affect the gene functional potential of different anammox species
69 still remains unclear (Shu et al., 2015). As anammox bacteria grow extremely slowly,
70 it may be meaningful to investigate the mixotrophic metabolism of anammox bacteria
71 further, as they may be acquiring extra energy from organic matter in order to grow
72 faster and thus shorten the reactor start-up period (Kartal et al., 2012).
73 Nutrient sources also affect metabolic interactions of the microbiome. Metabolic
74 interactions are ubiquitous in microbial communities, especially in microscale cell
75 aggregates, which play an important role in the functioning of microbial communities
76 (Cordero and Datta, 2016). From an ecological aspect, metabolic interactions may
77 help to maintain a stable coexistence between bacteria as a strategy to decrease the
78 energy consumption of the community (Guo et al., 2018; Pande et al., 2014). The
79 emergence and maintenance of metabolic interactions depends on many factors, such
80 as nutrient sources (Benomar et al., 2015) and spatial organization (Jiang et al., 2018).
81 Variation in nutrient conditions may influence gene transcription and thereby impact

metabolic interaction (Steffen et al., 2014). With the rapid development of meta-omics technology, the subject of metabolic interactions in microbial communities has drawn wide attention and turned into an important topic (Ponomarova and Patil, 2015). Pure anammox culture is extremely hard to obtain (Kuenen, 2008), and many heterotrophs, such as *Chloroflexi* and *Chlorobi,* are abundant in these communities (Speth et al., 2016). Recently, metabolic interactions which could perform energy-efficient nitrogen removal from wastewater, such as degradation of extracellular peptide substrates of anammox bacteria by heterotrophs and nitrogen and metabolite cross-feeding between anammox bacteria and heterotrophs, have been found in anammox consortia (Lawson et al., 2017). Cross-feeding is a kind of microbial interaction, in which metabolites could be shared by both the producer and the receiver, thus they can benefit from this process (Zhao et al., 2018). An investigative study of the mechanism underlying metabolic interactions in microbial communities may broaden our insight in regard to the composition and assembly of these communities (Zengler and Zaramela, 2018). However, the process by which organics influence interactions between anammox bacteria and heterotrophs in the consortia still remain unresolved.

We investigated competition between two typical anammox species, *J. caeni* and *B. sinica,* under autotrophic condition and mixotrophic condition with acetate addition based on batch tests. This phenotype was mapped to the underlying microbiome and further determined by sampling and analyzing autotrophic and mixotrophic anammox consortia. We characterized the gene functional potential, as well as the metabolic

network, using levels of anammox species in the anammox community, in order to explore the hypothesis that different anammox species have discrepant responses to acetate addition. As well, potential mechanisms associated with individual anammox species and their metabolic interactions in the consortia were analyzed. Our study provides a novel, detailed insight into mixotrophic metabolism of anammox bacteria, and suggests the possibility of predicting an increase in anammox performance under low C/N ratio.

2. Materials and methods

2.1 Sample collection

The anammox consortia used in this study was collected from a 3 L lab-scale sequencing batch reactor (SBR), which had been in operation at 37℃ for 280 days (Tang et al., 2018a). It was fed with a synthetic medium solution (Van de Graaf et al., 1995), and the concentration of NH_4^+-N and NO_2^--N in the influent were 300 mg L^{-1}. The hydraulic retention time (HRT) was 0.75 d. The pH was maintained at 6.8–7.5, and dissolved oxygen was removed by sparging with N_2-CO_2 (95/5%) gas. The batch tests were performed in six 250 mL serum bottles with the effective volume of 200 mL, each containing 0.315 g volatile suspended solids (VSS)/L anammox consortia inoculum mentioned above. By referring to the previous study about heterotrophic metabolism of anammox bacteria (Güven et al., 2005), the initial concentrations of NH_4^+-N and NO_2^--N in synthetic medium solution were set at a ratio of 1:1 with the concentrations of 50 mg L^{-1}. No sodium acetate was added (COD/TN=0) to the three

serum bottles of the control group (autotrophic group), while acetate was added to the three serum bottles of the experiment group (mixotrophic group), to maintain a final COD/TN ratio of 0.3 as per a previous study (Feng et al., 2018). The pH of the medium was adjusted to 7.2 by adding 0.1 M NaOH solution (Carvajal-Arroyo et al., 2014). Although the pH was not controlled, it was within a constant range of 7.2-7.5 during the experiment. After being sprayed with a gas mixture of N_2-CO_2 (95/5%) in order to maintain strict anaerobic conditions, all serum bottles were incubated at 37 ℃ and agitated at 150 rpm in the dark. 1 mL supernatant sample from each bottle were collected using syringes to determine the concentrations of NH_4^+-N, NO_2^--N, NO_3^--N and COD, which was done for five times during the experiment. At the point where the nitrate concentration between control and experiment group had statistical difference ($p < 0.05$ by t-test) and the difference of average nitrate concentration of control and experiment group was more than 10% (Kartal et al., 2007a), both autotrophic and mixotrophic anammox consortia were collected from each serum bottle and transferred into RNase-free tubes. After being rapidly frozen in liquid nitrogen, consortia samples were stored at -80 ℃ for subsequent metagenomic, metatranscriptomic, and metabolomic analyses, which could be applied to explore microbial gene functional potential and cross-feedings (Bahram et al., 2018; Lawson et al., 2017).

2.2 Metagenome and metatranscriptome sequencing

Autotrophic anammox consortia samples and mixotrophic anammox consortia

145 samples collected in triplicate from each bottle in batch tests were used for total DNA
146 extraction with the FastDNA Spin Kit for Soil (MP Biotechnology, CA, U.S.). DNA
147 concentration and purity was determined using TBS-380 and NanoDrop2000,
148 respectively. 1% agarose gels electrophoresis system was used to examine DNA
149 quality. Respective triplicate autotrophic and mixotrophic anammox consortia DNA
150 samples were mixed thoroughly for metagenome sequencing (Jia et al., 2018). Total
151 RNA was extracted from triplicate autotrophic and mixotrophic anammox consortia
152 samples from batch tests using the E.Z.N.A® Soil RNA Midi Kit (Omega BioTek,
153 Norcross, GA, U.S.) according to manufacturer's protocols. RNA quality was
154 assessed with a RNA6000 Nano chip (total RNA) in an Agilent 2100 Bioanalyzer and
155 was determined by the RNA integrity number (RIN). Respective triplicate autotrophic
156 and mixotrophic anammox consortia RNA samples were used for metatranscriptome
157 sequencing.
158 To construct paired-end library, DNA was fragmented to an average size of ~300 bp
159 with Covaris M220 (Gene Company Limited, China). Paired-end library was prepared
160 with TruSeqTM DNA Sample Prep Kit (Illumina, San Diego, CA, USA). Adapters
161 containing the full complement of sequencing primer hybridization sites were ligated
162 to the blunt-end fragments. Paired-end sequencing was accomplished on Illumina
163 HiSeq4000 platform (Illumina Inc., San Diego, CA, USA) at Majorbio Bio-Pharm
164 Technology Co., Ltd. (Shanghai, China) with HiSeq 3000/4000 PE Cluster Kit and
165 HiSeq 3000/4000 SBS Kits.

Total RNAs of consortia samples was subjected to an rRNA removal procedure with the Ribo-zero Magnetic kit according to the manufacturer's instruction (Epicentre, an Illumina® company). cDNA libraries were constructed with TruSeq™ RNA sample prep kit (Illumina). The barcoded libraries were paired end sequenced on the Illumina Hiseq 3000 platform at Majorbio Bio-Pharm Technology Co., Ltd. (Shanghai, China) with HiSeq 4000 PE Cluster Kit and HiSeq 4000 SBS Kits according to the manufacturer's instructions (www.illumina.com). Finally, raw metagenomics and metatranscriptomics datasets were deposited in the NCBI Sequence Read Archive database, and accession numbers were listed in Table S1.

2.3 Metagenomic assembly and binning

First, raw metagenomic reads were trimmed by stripping adaptor sequences and ambiguous nucleotides with SeqPrep version 1.1 based on default parameters (Prensner et al., 2011). The trimmed sequences were quality filtered with Sickle version 1.33 based on a minimum quality score of 20 and a minimum sequence length of 50 bp (Wu et al., 2016). Next, contigs and scaffolds were assembled individually for each sample via IDBA-UD with default parameters (Peng et al., 2012). Generated scaffolds were binned into draft genomes based on abundance and the tetranucleotide frequency using the MetaBAT version 0.32.5 with the sensitive model and a minimum contig size of 1500 bp (Kang et al., 2015). CheckM version 1.0.7 was employed to assess the completeness and the quality of recovered draft genomes through single-copy marker genes, which are specific within a phylogenetic lineage (Parks et

al., 2015). Draft genomes were deposited in GenBank, and accession numbers were listed in Table S2.

2.4 Phylogenetic analysis of recovered draft genomes

Phylosift version 1.0.1 was used to construct the phylogenetic tree (Darling et al., 2014). Marker genes of 37 reference genomes were selected. The concatenated protein alignments of the recovered draft genomes and reference genomes were aligned with MAFFT version 7.310 (Katoh et al., 2002) and concatenated again, using homemade scripts. Finally, a maximum likelihood phylogenetic tree was conducted using the RAxML version 8.2.11 (Stamatakis et al., 2008). Molecular Evolutionary Genetics Analysis (MEGA) software version 7.0 were used to visualize the phylogenetic tree (Kumar et al., 2016).

2.5 Metagenomic and metatranscriptomic analysis

First, raw metagenome reads of each sample were mapped to all contigs which were assembled into high-quality draft genomes (completeness ≥ 70% and contamination ≤ 10%) with the bbmap version 37.75 (minid = 0.95 and ambig = random). Then, the coverage of each bin was calculated by adding the reads which were mapped to the contigs of each bin and normalized by genome size.

The open reading frames (ORFs) of each recovered draft genome were annotated through Prodigal version 2.6.3 with the ‘meta’ option for metagenomes, where the minimum nucleotide length was set as 60 (Hyatt et al., 2010). ORFs were then queried against the carbohydrate-active enzymes database (CAZy, accessed on July

2016), the eggNOG database (accessed on December 2016) and Kyoto Encyclopedia of Genes and Genomes pathway database (KEGG, accessed on August 2017) with DIAMOND software, where the blast e value was set as 1e-5 (Buchfink et al., 2014). OrthoANI software was employed to calculate average nucleotide identity (Lee et al., 2016). Genome comparison was visualized via BLAST Ring Image Generator (BRIG) (Alikhan et al., 2011) and Easyfig software (Sullivan et al., 2011).

The raw metatranscriptomic reads were trimmed and quality filtered with the SeqPrep and Sickle software respectively. rRNA reads were removed through SortMeRNA version 2.0 (Kopylova et al., 2012) aligning to the SILVA 128 version database (accessed on February 2017). Non-rRNA reads were mapped to all contigs which were assembled into high-quality draft genomes with bbmap software. Read counts of each gene were calculated using htseq-count v0.9.1 with the 'intersection strict' parameter (Anders et al., 2015) and normalized as transcripts per million (TPM) values (Wagner et al., 2012). The relative gene expression and pathway expression were calculated by relativizing the median TPM across the draft genome, and by the median TPM value of each reaction in the pathway, respectively.

2.6 LC-MS-based metabolomic profiling and quantitation analysis

Metabolic products were extracted from the anammox consortia samples in autotrophic and mixotrophic groups. The protocols used to extract metabolic products were conducted according to those described previously (Guo et al., 2017; Tang et al., 2018b). In brief, anammox consortia suspension was collected by centrifugation,

washed using Phosphate buffer saline (PBS), and sonicated using a sonicator. Then, previously cooled methanol was added to the mixture, and the precipitated protein was removed by centrifugation. The supernatants were dried in a nitrogen gas stream. The residues were used to determine metabolite contents via LC-MS-based metabolomic analysis. All tests were conducted in quadruplicate.

3. Results

3.1 Higher nitrogen removal rate with acetate addition

In order to investigate the effect of acetate on the nitrogen removal rate of anammox consortia, batch tests were conducted. Based on nitrogen and chemical oxygen demand (COD) consumption (Fig. 1), 155 min was selected as the sludge sample collection point, for NO_3^--N concentrations in mixotrophic groups were significantly ($p < 0.05$ by t-test) and 40% lower than autotrophic groups at this point, which enabled the determination of discrepant expression genes and metabolic pathways of autotrophic and mixotrophic anammox consortia.

At 155 min, average NH_4^+-N removal rates were 311.5 ± 15.7 and 284.0 ± 7.2 mg N/(L•d), and the average NO_2^--N removal rates were 384.0 ± 41.9 and 359.2 ± 14.2 mg N/(L•d) in autotrophic group and mixotrophic group, respectively. Importantly, the average NO_3^--N accumulation rate in the mixotrophic group was 31.0 ± 19.0 mg N/(L•d), which was significantly lower than that in the autotrophic group (70.9 ± 8.0 mg N/(L•d)) ($p < 0.05$ by t-test). The ΔNO_3^--N/ΔNH_4^+-N ratio in the mixotrophic group (0.11 ± 0.06) was significantly lower compared to that of the autotrophic group

(0.23 ± 0.03) ($p < 0.05$). In mixotrophic group, a 59.0 ± 3.7 % COD was degraded by anammox consortia with a rate of 245.9 ± 12.4 mg/(L•d) until this point (Fig. 1(d)).

3.2 Draft genomes obtained by metagenomic binning

Sequencing of DNA extracted from autotrophic and mixotrophic anammox consortia yielded a total of 35,270,644 and 47,527,352 raw reads and 30,542,924 and 44,096,156 clean reads, respectively, after quality control. Next, the clean reads were assembled, and 124,673 and 152,645 contigs were generated with N50 of 2,215 bp and 2,391 bp. More than 85% of the quality filtered mRNA reads could be mapped to the assembly. After binning, 14 high-quality draft genomes (completeness ≥ 70%; contamination ≤ 10%) were obtained (Table 1) (Parks et al., 2015), making up 64-69% of the original sequencing reads. A phylogenetic tree of recovered draft genomes is shown (Fig. 2). Bacteria in the anammox community mainly belonged to the phyla *Planctomycetes*, *Chloroflexi*, *Proteobacteria* and *Cyanobacteria*, while an unclassified bacteria class (CPR1) was also detected. Further details regarding metagenomic and metatranscriptomic read mapping statistics are presented in Supplementary Data. Phylogenetic analysis showed that MAGs AMX1 and AMX2 were closely related to *J. caeni* and *B. sinica*, which shared average nucleotide identity values of 99.96% and 99.89% respectively. Circular maps of two draft genomes (AMX1 and AMX2) aligned to each other are shown in Fig. S1, and the nucleotide identity between them was 75.93%.

3.3 Prominent anammox species *B. sinica* and the gene functional potential with acetate addition

The bacterial relative abundance and gene expression levels were calculated using the transcripts per million (TPM) value (Moitinho-Silva et al., 2017). Anammox bacteria were highly enriched in the consortia, comprising approximately 55% of the whole community (Fig. S2). The six abundant species were *J. caeni* (AMX1 ~51%), *Rhodocyclaceae* (PRO1 ~20%), *Cyanobacteria* (CYA1 ~8%), *Anaerolineae* (CFX3 ~6%), *B. sinica* (AMX2 ~5%) and *Anaerolineae* (CFX2 ~2%). Gene expression abundance of *J. caeni* and *B. sinica* in the autotrophic group were 78.9 ± 2.7 % and 19.3 ± 2.6 % respectively, while these were 73.9 ± 4.9 % and 23.3 ± 4.5 %, respectively, in the mixotrophic groups. Interestingly, PRO1 was the only species whose gene expression abundance was significantly higher in the mixotrophic group compared to that in the autotrophic group ($p < 0.05$ by t-test).

In order to investigate the overall influences of acetate on *J. caeni* and *B. sinica*, genes with a significantly changed expression were selected and classified according to cluster orthologous gene (COG) function (Fig. S3). In *J. caeni*, expressions of a total of 284 genes were significantly down-regulated upon acetate addition, while 36 up-regulated genes were expressed. The main decreasing COG function observed in *J. caeni* was that of [C] energy production and conversion, containing 31 down-regulated genes. On the contrary, acetate greatly facilitated gene expression of *B. sinica* and a total of 1234 up-regulated genes were expressed. Abundant, increasing

COG functions in *B. sinica* included [C] energy production and conversion (105 significantly up-regulated genes expressed), [E] amino acid transport and metabolism (81 significantly up-regulated genes expressed) and [J] translation, ribosomal structure and biogenesis (76 significantly up-regulated genes expressed).

N-cycle-related functional genes (*hdh, hzs, hao, nar, nir and nrf*) were found to be highly expressed in anammox bacteria. By comparing TPM values in *J. caeni* and *B. sinica*, between the autotrophic and mixotrophic groups, it was observed that transcription level of *nrfA* for DNRA function in *B. sinica* was significantly up-regulated in the presence of acetate (fold change = 1.79, $p < 0.01$), but no significant difference of *nrfA* expression was found in *J. caeni* (fold change = 0.95, $p > 0.05$). TPM values of *nrfA* in *B. sinica* was 6363–14565, which was higher than that in *J. caeni* (TPM value = 208–231) by nearly 1 to 2 orders of magnitude. No significant difference was found between the expression levels of other functional genes mentioned above, in the anammox bacteria of the two groups. Denitrification genes, including *narG, narZ, nxrA, nirS, nosZ and napA*, were detected in bacteria of the anammox consortia. Genes expression of *narG, narZ, nxrA* in CFX2 (fold change = 2.11, $p < 0.05$ by t-test), *nirS* in CFX3 (fold change = 5.06, $p < 0.01$ by t-test), *nosZ* in CYA1 (fold change = 3.72, $p < 0.01$ by t-test) and *napA* in PRO1 (fold change = 2.11, $p < 0.05$ by t-test) were stimulated by acetate.

Importantly, genes involved in acetate transformation were selected to analyze acetate metabolism by anammox consortia. Acetate was transformed mainly through

three distinct routes (Fig. 3). The first route involved two types of acetyl-CoA synthetases (Acs), AMP-forming Acs (AMP-Acs) (EC 6.2.1.1) and ADP-forming Acs (ADP-Acs) (EC 6.2.1.13), which could catalyze acetate to form acetyl-CoA. AMP-*acs* expression level was up-regulated significantly with acetate addition in *B. sinica* (fold change = 1.78, $p < 0.01$ by t-test) and PRO1 (fold change = 5.93, $p < 0.05$ by t-test). Comparative genome analysis indicated that a response regulator, *atoC* was located up-stream of AMP-*acs* in *B. sinica*, but none was found in the proximity of AMP-*acs* in *J. caeni* (Fig. S4). Expression of *atoC* in *B. sinica* was significantly up-regulated with acetate addition (fold change = 1.92, $p < 0.05$ by t-test), but it did not change significantly in *J. caeni*. cAMP receptor protein (CRP), which encodes *acs* transcription factor, was found in *B. sinica* and was up-regulated with acetate addition (fold change = 2.02, $p < 0.01$ by t-test), but it was missing in *J. caeni*. The second route is composed of aldehyde dehydrogenase (ALDH, EC 1.2.1.3) catalyzing the reversible reaction of acetate to acetaldehyde. This gene was detected in *B. sinica*, *J. caeni*, CFX2, CFX3 and CYA1, but was found expressing more only in CFX3 with acetate addition (fold change = 2.15, $p < 0.05$ by t-test). The third route was dependent on acetate kinase (AckA, EC 2.7.2.1) and D-xylulose-5-phosphate phosphoketolase (Xfp, EC 4.1.2.9), and termed AckA-Xfp pathway. The first step was the transformation of acetate to acetyl phosphate. Gene *ackA* only existed in *B. sinica* and PRO1. Acetyl phosphate in *B. sinica* could be further transformed to D-Xylulose 5-phosphate, catalyzed by Xfp. Thus, acetate metabolism pathways in *B. sinica* were

more versatile than those in *J. caeni*.

3.4 Strengthened amino acid cross-feeding in anammox consortia with acetate

Previous studies indicate that amino acid exchange occurs in microbial communities, as a type of important inter-species interaction (Embree et al., 2015; Lawson et al., 2017). Therefore, the effect of acetate on amino acid exchange in anammox community was investigated. Expression levels of 20 amino acid synthetic and degradation pathways in six abundant bacteria are shown (Fig. 4 (a) and (b)). Among six abundant bacteria species, only PRO1 had intact synthetic pathways of all 20 amino acids. Interestingly, TPM values of many amino acids synthetic pathways were significantly increased with acetate addition ($p < 0.05$), especially for PRO1 and *B. sinica*. For CFX2, amino acids tryptophan (Trp), phenylalanine (Phe), histidine (His), lysine (Lys) and arginine (Arg) could not be synthesized independently, but their degradation pathways were found in the genome, and the expression of Lys and Arg degradation pathways were significantly up-regulated in CFX2 with acetate addition (fold change (Lys) = 1.78, fold change (Arg) = 1.55). Meanwhile, the synthetic pathways of Lys and Arg were significantly up-regulated in PRO1 and *B. sinica* in the presence of acetate (Fig. 4(a)). For CYA1, synthetic pathways of amino acids Trp, Tyr, His, methionine (Met), proline (Pro) and serine (Ser) were lacking, but degradation pathways of these amino acids were found in the genome, and the expression of Trp, Tyr and Met degradation pathways were up-regulated significantly, with fold changes of 2.48, 1.82 and 1.96, respectively. Genes encoding extracellular,

outer membrane and periplasmic peptidase involved in extracellular protein degradation, except the periplasmic peptidase of AMX1 and extracellular peptidase of PRO1, were detected in all six abundant bacteria in the community (Fig. 4(d)). The total expression of these peptidase genes were significantly up-regulated in CFX2, PRO1 and *B. sinica* ($p < 0.05$). Genes involved in amino acid and oligopeptide transport system were also detected (Fig. 4(e)), and the genes expression levels were significantly promoted by acetate in CFX2, CYA1 and PRO1 ($p < 0.05$).

Metabolomic analysis was conducted to evaluate metabolites contents of the whole consortia. A total of 18 amino acids were detected (Fig. S5), and 10 amino acids including Met and isoleucine (Ile), were up-regulated significantly with acetate addition, which corresponded to the gene expression profile in the consortia.

3.5 Strengthened vitamin cross-feeding in anammox consortia with acetate

It has been reported that some heterotrophic bacteria in anammox consortia lacked key genes to synthesize B-vitamin (Lawson et al., 2017), which were confirmed in this study. Key genes for thiamine (vitamin B1) synthesis (hydroxymethylpyrimidine/ phosphomethylpyrimidine kinase etc.) and biotin (vitamin B7) synthesis (biotin synthase etc.) were missing in the CFX2, CFX3 and CYA1 genomes, while *J. caeni*, *B. sinica* and PRO1 had intact vitamin B1 and vitamin B7 synthetic pathways (Fig. 4(c)). For the vitamin B1 synthetic pathway in the autotrophic group, TPM values were 420.3 ± 46.9, 294.7 ± 71.5 and 2.5 ± 0.2 in *J. caeni*, *B. sinica* and PRO1, respectively. In the mixotrophic group, TPM value of vitamin B1 synthetic pathway of *B. sinica*

was 548.0 ± 81.6, even higher than that of *J. caeni* (345.8 ± 57.6). Therefore, acetate significantly promoted the expression of genes involved in vitamin B1 synthetic pathways in *B. sinica* and PRO1 ($p < 0.05$). In regard to vitamin B7 synthesis, acetate significantly promoted the expression of key genes such as adenosylmethionine-8-amino-7-oxononanoate aminotransferase (EC 2.6.1.62) in *B. sinica* and PRO1 ($p < 0.05$). Additionally, intact vitamin B12 synthetic pathways were only found in *B. sinica* and PRO1, where their relative expressions were significantly up-regulated with the addition of acetate ($p < 0.05$).

4. Discussion

4.1 Metagenomics analysis indicates different acetate metabolic pathways in *B. sinica* and *J. caeni*

Since anammox bacteria are able to use acetate rather than glucose, methanol, and alcohol as carbon source (Du et al., 2017; Güven et al., 2005), and acetate is one of the widest external carbon sources for denitrification at wastewater treatments (Du et al., 2017; Gong et al., 2013), many studies have focused on the use of acetate by anammox bacteria. The leading hypothesis contends that acetate or other fatty acids may be oxidized by nitrate (electron acceptor), where nitrate is then possibly reduced via the DNRA pathway (Guven et al., 2005; Kartal et al., 2007a, 2007b). Based on $\delta^{13}C$ values of lipids and substrates, it was speculated that acetate was not directly incorporated into the biomass, but first degraded into CO_2 and then fixed via the acetyl-CoA pathway (Kartal et al., 2008). In fact, it is reported that different anammox

consortia may behave discrepantly under acetate stress (Huang et al., 2014; Kartal et al., 2008). Therefore, it may be helpful to explore potential discrepancies in gene expression among different anammox species during the acetate oxidation process.

Based on metagenomics and metatranscriptomics analysis, we discovered three distinct routes for acetate transformation in anammox bacteria. Considering that anammox bacteria had the highest abundance and highest expression levels of genes related with acetate metabolism (Fig. 3 and Supplementary Data), the acetate was mainly metabolized by anammox bacteria rather than denitrifying bacteria. Compared to *J. caeni*, *B. sinica* was more capable of acetate and acetyl-CoA transformation, and acetate metabolic pathways of *B. sinica* were more versatile, conferring a competitive advantage to *B. sinica* in a mixotrophic environment. Acetyl-CoA pathway is a common route for acetate transformation in bacteria (Krivoruchko et al., 2015). Both *B. sinica* and *J. caeni* possess AMP-Acs and ADP-Acs. Both these enzymes are capable of catalyzing acetate into acetyl-CoA, but via different mechanisms, as ADP-Acs catalyzes the synthesis of acetyl-CoA from acetate in a single step, while AMP-Acs synthesizes it in two steps (Starai and Escalante-Semerena, 2004). And the AMP-Acs route is a high affinity pathway, as the K_m for acetate was 200 μM and the reaction occurs at a low acetate concentration (Krivoruchko et al., 2015). Discrepancies in AMP-*acs* between the two anammox bacteria may be one significant reason for their response to acetate being different. First, the TPM values of AMP-*acs* in *B. sinica* (1629.8–2020.9) were almost an order of magnitude higher than that in *J.*

caeni (126.0–206.0) (Fig. 3), indicating more acetate might be transformed by *B. sinica* via this pathway. Secondly, the expression level of AMP-*acs* was significantly up-regulated in *B. sinica* in the presence of acetate; whereas the presence of acetate did not change the AMP-*acs* expression of *J. caeni*, demonstrating that AMP-*acs* regulation in *B. sinica* was more sensitive to acetate than in *J. caeni*. Thus, it may be suggested that more acetyl-CoA was generated from acetate. Acetyl-CoA plays a central role in cellular metabolism, serving as a crucial precursor of many metabolites such as fatty acids and vitamins, and participating in the TCA cycle, which is associated with the synthesis of amino acids, nucleotide bases and porphyrins (Krivoruchko et al., 2015). Therefore, we postulate that acetate may directly regulate the acetyl-CoA pathway, which then further influences other metabolic processes in the anammox bacteria.

Additionally, there may be three acetate metabolic pathways in *B. sinica*, compared to only two in *J. caeni*. The route which is present in *B. sinica* was the AckA-Xfp pathway, which has been reported in bacteria as well as in fungi (Ingram-Smith et al., 2006). Although TPM values of genes in *B. sinica* involved in AckA-Xfp pathway did not change significantly with the addition of acetate, this pathway may also contribute to acetate consumption of *B. sinica*. Therefore, *B. sinica* may be more adapted to a mixotrophic lifestyle than *J. caeni*. Of course, the roles of ALDH and AckA-Xfp pathways in anammox bacteria in metabolizing other kinds of organic carbons should be further investigated.

4.2 *J. caeni* and *B. sinica* display different acetate regulatory mechanisms

Discrepancies in genome structure and gene content between *B. sinica* and *J. caeni* may lead to differences in gene transcription in response to environmental stimuli. AtoC belongs to the NtrC family, and plays a positive role in regulating the uptake of short-chain fatty acids (Rhie and Dennis, 1995). Although both *B. sinica* and *J. caeni* contain *atoC*, it is located near AMP-*acs* and significantly up-regulated with the addition of acetate in *B. sinica*, which may have a facilitating effect on AMP-*acs* expression (Van de Vossenberg et al., 2013). Even further, AMP-*acs* regulatory mechanism is a complex system, where CRP is an important factor, that may activate the major *acs* promoter, acsP2 (Starai and Escalante-Semerena, 2004; Wolfe, 2005). The process of acetate metabolism in *B. sinica* is likely regulated by CRP, and a lack of CRP may affect the acetate uptake process of *J. caeni*. It was reported that the expression of N-cycle related functional genes in the anammox consortia may also be affected by organics (Shu et al., 2015). In our study, *nrfA* expression was significantly up-regulated in *B. sinica* with acetate addition, suggesting that the DNRA process was promoted, which was consistent with the results of batch tests. It has been found that *nrfA* expression may also be regulated by CRP in Shewanella (Dong et al., 2012). Therefore, CRP may play an important role in mixotrophic and nitrogen metabolism of *B. sinica*, and its contribution in nitrogen removal needs to be further explored in sewage treatment. The expression levels of functional genes involved in the anammox process, such as *hzs*, *hdh*, and *nxrA*, were not affected significantly by acetate in the

anammox consortia. It may be due to the fact the experimental period was too brief for these genes to exhibit significantly different expression levels between autotrophic and mixotrophic groups, as the expression levels of these genes were depended on the growth rate of anammox bacteria (Klumpp and Hwa 2014; Park et al., 2010). Meanwhile, since expression levels of nitrogen metabolism genes were consistent with the substrate concentrations (Wang et al., 2016), the similar expression levels of these genes in control and experiment groups could also be caused by the same nitrogen concentrations in these two groups.

Overall, COG functions analysis of integrated changes of gene expression indicated that *B. sinica* was more competitive than *J. caeni* with acetate addition. The process of [C] energy production and conversion was most affected in both *J. caeni* and *B. sinica*, where more specifically, it was inhibited in *J. caeni* and promoted in *B. sinica*. This may be directly reflected in the metabolic activity of these bacteria. Many genes belonging to COG function [O], posttranslational modification, protein turnover, and chaperones, were up-regulated in *J. caeni*, indicating that the mixotrophic culture was not appropriate, and needed to cope with acetate stress. As for *B. sinica*, expressions of more than 70 genes of COG function [J], translation, ribosomal structure, and biogenesis, were up-regulated, indicating that acetate favorably induced reproduction and growth of *B. sinica*. Therefore, *B. sinica* was more competitive than *J. caeni* bacteria under mixotrophic conditions, which was in accordance with previous studies (Feng et al., 2018; Kartal et al., 2008).

4.3 Role of acetate in regulating metabolic cross-feedings between *B. sinica* and heterotrophs in order to conserve metabolic energy

Since an anammox consortium is a complex microbial community, interactions between anammox bacteria and other heterotrophic bacteria should not be neglected when analyzing community functions. In this study, we detected that a variety of heterotrophs were present in the anammox consortia, including *Chloroflexi bacterium* (CFX2), *Anaerolineae bacterium* (CFX3), *Rhodocyclaceae bacterium* (PRO1) and *Cyanobacteria* (CYA1) among others. As acetate could be used by both anammox bacteria and heterotrophs, microbial competition for substrate would be introduced by acetate (Cao et al., 2017; Huang et al., 2014). Here, we mainly focused on metabolic exchanges between anammox bacteria and heterotrophs (Fig. 5). Firstly, expression levels of the denitrification genes in CFX2, CFX3, CYA1 and PRO1, mentioned above, were up-regulated with the addition of acetate. Meanwhile, the expression of *nrfA* in *B. sinica* was enhanced significantly when adding acetate, indicating more NO_3^--N may be consumed through the DNRA process in *B. sinica*. Thus, acetate could enhance the nitrogen cycle, and further improve the nitrogen removal rate, which has been confirmed in the long-term reactor operation process (Feng et al., 2018).

Amino acids cross-feeding between *B. sinica* and heterotrophs in anammox community could also be promoted by acetate addition, contributing to metabolic energy cost saving of the whole community (Pande et al., 2014). Metatranscriptomics

501 analysis of gene expression profile in each abundant bacterial species, indicates that
502 heterotrophs, such as *Chloroflexi bacteria* (CFX2, CFX3), may be able to degrade the
503 extracellular peptides excreted by anammox bacteria. We detected that peptidase and
504 amino acid transporters were located in the extracellular region, the membrane or in
505 the periplasm of heterotrophic bacteria. Parts of the amino acid synthetic pathway,
506 especially those with a high biosynthetic cost, were lacking in some bacteria. Thus,
507 they could obtain the required amino acids directly from anammox bacteria or others
508 by degrading EPS. Although the dominant heterotrophs in anammox consortia were
509 different than the *Chlorobi* bacteria in the previous study (Lawson et al., 2017), their
510 ecological role and function in the community appears to be similar. Amino acid
511 exchange is a type of metabolic cross-feeding, regarded as an evolutionarily
512 optimizing strategy which aids in reducing the bacterial metabolic burden (Mee et al.,
513 2014). In this study, induced by high expression level of AMP-*acs*, *B. sinica* may
514 synthesize more acetyl-CoA from acetate, which could further facilitate amino acids
515 production (Krivoruchko et al., 2015). Our results also indicated that the expression
516 levels of certain amino acid synthetic pathways were up-regulated significantly in *B.*
517 *sinica*, such as synthetic pathways of Lys and Arg. Therefore, acetate may enhance
518 metabolic cross-feeding between *B. sinica* and heterotrophs. A more active, but costly,
519 amino acid cross-feeding may result in more energy being saved for use in increasing
520 the biomass (Guo et al., 2018).
521 Besides, B-vitamin metabolic exchange between *B. sinica* and heterotrophs in

anammox consortia could also be enhanced by acetate addition, helping to conserve energy by reducing metabolic energy costs. Synthetic pathway integrity and TPM values indicate that *B. sinica* and *J. caeni* may act as the main suppliers of vitamin B1 and vitamin B7 to other members of the community. *B. sinica* also had intact vitamin B12 synthetic pathways so that vitamin B12 might be supplied by *B. sinica*. As acetyl-CoA is precursor of vitamins, acetate might promote B-vitamin synthesis in *B. sinica* via up-regulating synthesis of acetyl-CoA, and may facilitate the B-vitamin exchange process in the community (Krivoruchko et al., 2015). B-vitamins are a large group of cofactors, which are essential for the metabolism and growth of all microbes (Jaehme and Slotboom, 2015). However, the cost of their synthesis is high. Therefore, sharing of B-vitamins or their precursors between community members may help to reduce metabolic energy costs, which may be accomplished via acetate addition (Romine et al., 2017).

5. Conclusions

In this study, discrepant responses of anammox species *J. caeni* and *B. sinica*, and metabolic interactions within anammox consortia, in response to acetate addition were investigated. According to COG functions analysis, *B. sinica* was more competitive than *J. caeni* when adding acetate. *B. sinica* exhibited superiority in metabolic activity and growth compared to *J. caeni*, due to the up-regulation of numerous genes that act on metabolic processes. Three acetate metabolic pathways were found in *B. sinica*, including acetyl-CoA pathway, ALDH pathway and AckA-Xfp pathway, but only the

first two were observed in *J. caeni*. Discrepancies in the acetate metabolic pathways and *AMP-acs* expression regulated by CRP, which exist between two anammox species, may result in different responses to acetate. Importantly, metabolic cross-feeding, including the nitrogen cycle, amino acid cross-feeding and B-vitamin metabolic exchange were enhanced, especially between *B. sinica* and other heterotrophs, with acetate addition, contributing to a reduction in metabolic energy cost to the whole community, in addition to improving nitrogen removal rates of the anammox consortia.

Supplementary materials

Word document

Accession numbers of metagenomic and metatranscriptomic sequencing data **(Table S1).** Metagenome-assembled genome (MAG) GenBank accession numbers **(Table S2).** Circular maps showing comparative genome analysis between *B. sinica* and *J. caeni* **(Figure S1).** Abundance and gene expression of each bacteria in anammox consortia **(Figure S2).** Numbers of significantly different gene transcripts between autotrophic and mixotrophic groups of each COG function categories in *J. caeni* and *B. sinica* **(Figure S3).** Comparative genomics analysis of ACS (AMP-forming) gene and its nearby genes between *J. caeni* and *B. sinica* **(Figure S4).** Amino acids contents (Z score) in autotrophic and mixotrophic anammox consortia quantified by LC-MS based metabolomics **(Figure S5).**

Excel document

Metagenomic and metatranscriptomic read mapping statistics **(Supplementary Data)**.

Corresponding author

E-mail: liusitong@pku.edu.cn (Sitong LIU)

Notes

The authors declare no competing financial interests.

Acknowledgments

The authors are grateful to the National Natural Science Foundations of China (No. 51878008 and 91647211) for financial support. The financial support from Yellow River Institute of Hydraulic Research (No. HKY-JBYW-2016-01) are also highly appreciated.

References

Alikhan, N.F., Petty, N.K., Ben Zakour, N.L., Beatson, S.A., 2011. BLAST Ring Image Generator (BRIG): Simple prokaryote genome comparisons. BMC Genomics 12, 402.

Anders, S., Pyl, P.T., Huber, W., 2015. HTSeq-A Python framework to work with high-throughput sequencing data. Bioinformatics 31, 166–169.

Bahram, M., Hildebrand, F., Forslund, S.K., Anderson, J.L., Soudzilovskaia, N.A., Medema, M.H., Maltz, M.R., Mundra, S., Olsson, P.A., Pent, M., Põlme, S., Sunagawa, S., 2018. Structure and function of the global topsoil microbiome. Nature 560, 233–237.

Benomar, S., Ranava, D., Cárdenas, M.L., Trably, E., Rafrafi, Y., Ducret, A., Hamelin, J., Lojou, E., Steyer, J.P., Giudici-Orticoni, M.T., 2015. Nutritional stress induces exchange of cell material and energetic coupling between bacterial species. Nat. Commun. 6, 6283.

Bombar, D., Heller, P., Sanchez-Baracaldo, P., Carter, B.J., Zehr, J.P., 2014. Comparative genomics reveals surprising divergence of two closely related strains of uncultivated UCYN-A cyanobacteria. ISME J. 8, 2530–2542.

Buchfink, B., Xie, C., Huson, D.H., 2014. Fast and sensitive protein alignment using DIAMOND. Nat. Methods 12, 59–60.

Cao, Y., van Loosdrecht, M.C.M., Daigger, G.T., 2017. Mainstream partial nitritation–anammox in municipal wastewater treatment: status, bottlenecks, and further studies. Appl. Microbiol. Biotechnol. 1365–1383.

Carvajal-Arroyo, J.M., Puyol, D., Li, G., Swartwout, A., Sierra-Álvarez, R., Field, J.A., 2014. Starved anammox cells are less resistant to NO_2^- inhibition. Water Res. 65, 170–176.

Cordero, O.X., Datta, M.S., 2016. Microbial interactions and community assembly at microscales. Curr. Opin. Microbiol. 31, 227–234.

599 Darling, A.E., Jospin, G., Lowe, E., Matsen, F.A., Bik, H.M., Eisen, J.A., 2014. PhyloSift:
600 phylogenetic analysis of genomes and metagenomes. PeerJ 2, e243.

601 Dong, Y., Wang, J., Fu, H., Zhou, G., Shi, M., Gao, H., 2012. A Crp-dependent two-component system
602 regulates nitrate and nitrite respiration in Shewanella oneidensis. PLoS One 7.

603 Du, R., Cao, S., Li, B., Niu, M., Wang, S., Peng, Y., 2017. Performance and microbial community
604 analysis of a novel DEAMOX based on partial-denitrification and anammox treating ammonia
605 and nitrate wastewaters. Water Res. 108, 46–56.

606 Embree, M., Liu, J.K., Al-Bassam, M.M., Zengler, K., 2015. Networks of energetic and metabolic
607 interactions define dynamics in microbial communities. Proc. Natl. Acad. Sci. 112,
608 15450–15455.

609 Feng, Y., Zhao, Y., Guo, Y., Liu, S., 2018. Microbial transcript and metabolome analysis uncover
610 discrepant metabolic pathways in autotrophic and mixotrophic anammox consortia. Water Res.
611 128, 402–411.

612 Gong, L., Huo, M., Yang, Q., Li, J., Ma, B., Zhu, R., Wang, S., Peng, Y., 2013. Performance of
613 heterotrophic partial denitrification under feast-famine condition of electron donor: A case study
614 using acetate as external carbon source. Bioresour. Technol. 133, 263–269.

615 Guo, Y., Liu, S., Tang, X., Wang, C., Niu, Z., Feng, Y., 2017. Insight into c-di-GMP regulation in
616 anammox aggregation in response to alternating feed loadings. Environ. Sci. Technol. 51,
617 9155–9164.

618 Guo, Y., Zhao, Y., Zhu, T., Li, J., Feng, Y., Zhao, H., Liu, S., 2018. A metabolomic view of how low
619 nitrogen strength favors anammox biomass yield and nitrogen removal capability. Water Res.
620 143, 387–398.

621 Guven, D., Dapena, A., Kartal, B., Schmid, M.C., Maas, B., van de Pas-Schoonen, K., Sozen, S.,
622 Mendez, R., Op den Camp, H.J., Jetten, M.S.M., Strous, M., Schmidt, I., 2005. Propionate
623 oxidation by and methanol inhibition of anaerobic ammonium-oxidizing bacteria. Appl Env.

624 Microbiol 71, 1066–1071.

625 Huang, X.L., Gao, D.W., Tao, Y., Wang, X.L., 2014. C2/C3 fatty acid stress on anammox consortia
626 dominated by Candidatus Jettenia asiatica. Chem. Eng. J. 253, 402–407.

627 Hyatt, D., Chen, G.L., LoCascio, P.F., Land, M.L., Larimer, F.W., Hauser, L.J., 2010. Prodigal:
628 Prokaryotic gene recognition and translation initiation site identification. BMC Bioinformatics 11,
629 119.

630 Ingram-Smith, C., Martin, S.R., Smith, K.S., 2006. Acetate kinase: not just a bacterial enzyme. Trends
631 Microbiol. 14, 249–253.

632 Jaehme, M., Slotboom, D.J., 2015. Diversity of membrane transport proteins for vitamins in bacteria
633 and archaea. Biochim. Biophys. Acta - Gen. Subj. 1850, 565–576.

634 Jenni, S., Vlaeminck, S.E., Morgenroth, E., Udert, K.M., 2014. Successful application of
635 nitritation/anammox towastewater with elevated organic carbon to ammonia ratios. Water Res.
636 49, 316–326.

637 Jia, Y., Khanal, S.K., Shu, H., Zhang, H., Chen, G.H., Lu, H., 2018. Ciprofloxacin degradation in
638 anaerobic sulfate-reducing bacteria (SRB) sludge system: Mechanism and pathways. Water Res.
639 136, 64–74.

640 Jiang, X., Zerfaß, C., Feng, S., Eichmann, R., Asally, M., Schäfer, P., Soyer, O.S., 2018. Impact of
641 spatial organization on a novel auxotrophic interaction among soil microbes. ISME J.
642 1443–1456.

643 Kang, D.D., Froula, J., Egan, R., Wang, Z., 2015. MetaBAT, an efficient tool for accurately
644 reconstructing single genomes from complex microbial communities. PeerJ 3, e1165.

645 Kartal, B., Kuenen, J.G., van Loosdrecht, M.C.M., 2010. Sewage treatment with anammox. Science
646 328(5979), 702–703.

647 Kartal, B., Kuypers, M.M.M., Lavik, G., Schalk, J., Op Den Camp, H.J.M., Jetten, M.S.M., Strous, M.,

2007a. Anammox bacteria disguised as denitrifiers: Nitrate reduction to dinitrogen gas via nitrite and ammonium. Environ. Microbiol. 9, 635–642.

Kartal, B., Rattray, J., van Niftrik, L.A., van de Vossenberg, J., Schmid, M.C., Webb, R.I., Schouten, S., Fuerst, J.A., Damsté, J.S., Jetten, M.S.M., Strous, M., 2007b. Candidatus "Anammoxoglobus propionicus" a new propionate oxidizing species of anaerobic ammonium oxidizing bacteria. Syst. Appl. Microbiol. 30, 39–49.

Kartal, B., van Niftrik, L., Keltjens, J.T., Op den Camp, H.J.M., Jetten, M.S.M., 2012. Anammox-Growth Physiology, Cell Biology, and Metabolism, 1st ed, Advances in Microbial Physiology. Elsevier Ltd.

Kartal, B., Van Niftrik, L., Rattray, J., Van De Vossenberg, J.L.C.M., Schmid, M.C., Sinninghe Damsté, J., Jetten, M.S.M., Strous, M., 2008. Candidatus "Brocadia fulgida": An autofluorescent anaerobic ammonium oxidizing bacterium. FEMS Microbiol. Ecol. 63, 46–55.

Katoh, K., Misawa, K., Kuma, K., Miyata, T., 2002. MAFFT: a novel method for rapid multiple sequence alignment based on fast Fourier transform. Nucleid Acid Res. 30, 3059–3066.

Kim, S., Park, J. eun, Cho, Y.B., Hwang, S.J., 2013. Growth rate, organic carbon and nutrient removal rates of Chlorella sorokiniana in autotrophic, heterotrophic and mixotrophic conditions. Bioresour. Technol. 144, 8–13.

Klumpp, S., Hwa, T., 2014. Bacterial growth: Global effects on gene expression, growth feedback and proteome partition. Curr. Opin. Biotechnol. 28, 96–102.

Kopylova, E., Noé, L., Touzet, H., 2012. SortMeRNA: Fast and accurate filtering of ribosomal RNAs in metatranscriptomic data. Bioinformatics 28, 3211–3217.

Krivoruchko, A., Zhang, Y., Siewers, V., Chen, Y., Nielsen, J., 2015. Microbial acetyl-CoA metabolism and metabolic engineering. Metab. Eng. 28, 28–42.

Kuenen, J.G., 2008. Anammox bacteria: from discovery to application. Nat. Rev. Microbiol. 6,

320–326.

Kumar, S., Stecher, G., Tamura, K., 2016. MEGA7: Molecular Evolutionary Genetics Analysis Version 7.0 for Bigger Datasets. Mol. Biol. Evol. 33, 1870–1874.

Lawson, C.E., Wu, S., Bhattacharjee, A.S., Hamilton, J.J., Mcmahon, K.D., Goel, R., Noguera, D.R., 2017. Metabolic network analysis reveals microbial community interactions in anammox granules. Nat. Commun. 8, 15416.

Le, C., Stuckey, D.C., 2016. Colorimetric measurement of carbohydrates in biological wastewater treatment systems: A critical evaluation. Water Res. 94, 280–287.

Leal, C.D., Pereira, A.D., Nunes, F.T., Ferreira, L.O., Coelho, A.C.C., Bicalho, S.K., Mac Conell, E.F.A., Ribeiro, T.B., de Lemos Chernicharo, C.A., de Araújo, J.C., 2016. Anammox for nitrogen removal from anaerobically pre-treated municipal wastewater: Effect of COD/N ratios on process performance and bacterial community structure. Bioresour. Technol. 211, 257–266.

Lee, I., Kim, Y.O., Park, S.C., Chun, J., 2016. OrthoANI: An improved algorithm and software for calculating average nucleotide identity. Int. J. Syst. Evol. Microbiol. 66, 1100–1103.

Mee, M.T., Collins, J.J., Church, G.M., Wang, H.H., 2014. Syntrophic exchange in synthetic microbial communities. Proc. Natl. Acad. Sci. 111, E2149–E2156.

Moitinho-Silva, L., Díez-Vives, C., Batani, G., Esteves, A.I.S., Jahn, M.T., Thomas, T., 2017. Integrated metabolism in sponge-microbe symbiosis revealed by genome-centered metatranscriptomics. ISME J. 11, 1651–1666.

Pande, S., Merker, H., Bohl, K., Reichelt, M., Schuster, S., De Figueiredo, L.F., Kaleta, C., Kost, C., 2014. Fitness and stability of obligate cross-feeding interactions that emerge upon gene loss in bacteria. ISME J. 8, 953–962.

Park, H., Rosenthal, A., Ramalingam, K., Fillos, J., Chandran, K., 2010. Linking community profiles, gene expression and n-removal in anammox bioreactors treating municipal anaerobic digestion

reject water. Environ. Sci. Technol. 44, 6110–6116.

Parks, D.H., Imelfort, M., Skennerton, C.T., Hugenholtz, P., Tyson, G.W., 2015. CheckM: assessing the quality of microbial genomes recovered from. Cold Spring Harb. Lab. Press Method 1, 1–31.

Peng, Y., Leung, H.C.M., Yiu, S.M., Chin, F.Y.L., 2012. IDBA-UD: A de novo assembler for single-cell and metagenomic sequencing data with highly uneven depth. Bioinformatics 28, 1420–1428.

Ponomarova, O., Patil, K.R., 2015. Metabolic interactions in microbial communities: Untangling the Gordian knot. Curr. Opin. Microbiol. 27, 37–44.

Prensner, J.R., Iyer, M.K., Balbin, O.A., Dhanasekaran, S.M., Cao, Q., Brenner, J.C., Laxman, B., Asangani, I.A., Grasso, C.S., Kominsky, H.D., Cao, X., Jing, X., Wang, X., Siddiqui, J., Wei, J.T., Robinson, D., Iyer, H.K., Palanisamy, N., Maher, C.A., Chinnaiyan, A.M., 2011. Transcriptome sequencing across a prostate cancer cohort identifies PCAT-1, an unannotated lincRNA implicated in disease progression. Nat. Biotechnol. 29, 742–749.

Rhie, H.G., Dennis, D., 1995. Role of fadR and atoC(Con) mutations in poly(3-hydroxybutyrate-co-3-hydroxyvalerate) synthesis in recombinant *pha+ Escherichia coli*. Appl. Environ. Microbiol. 61, 2487–2492.

Romine, M.F., Rodionov, D.A., Maezato, Y., Osterman, A.L., Nelson, W.C., 2017. Underlying mechanisms for syntrophic metabolism of essential enzyme cofactors in microbial communities. ISME J. 11, 1434–1446.

Shu, D., He, Y., Yue, H., Zhu, L., Wang, Q., 2015. Metagenomic insights into the effects of volatile fatty acids on microbial community structures and functional genes in organotrophic anammox process. Bioresour. Technol. 196, 621–633.

Smith, A.L., Kelly, D.P., Wood, A.P., 1980. Metabolism of Thiobacillus A2 grown under autotrophic, mixotrophic and heterotrophic conditions in chemostat culture. J. Gen. Microbiol. 121, 127–138.

720 Speth, D.R., in 't Zandt, M.H., Guerrero-Cruz, S., Dutilh, B.E., Jetten, M.S.M., 2016. Genome-based
721 microbial ecology of anammox granules in a full-scale wastewater treatment system. Nat.
722 Commun. 7, 11172.

723 Stamatakis, A., Hoover, P., Rougemont, J., 2008. A rapid bootstrap algorithm for the RAxML web
724 servers. Syst. Biol. 57, 758–771.

725 Starai, V.J., Escalante-Semerena, J.C., 2004. Acetyl-coenzyme A synthetase (AMP forming). Cell. Mol.
726 Life Sci. 61, 2020–2030.

727 Steffen, M.M., Dearth, S.P., Dill, B.D., Li, Z., Larsen, K.M., Campagna, S.R., Wilhelm, S.W., 2014.
728 Nutrients drive transcriptional changes that maintain metabolic homeostasis but alter genome
729 architecture in Microcystis. ISME J. 8, 1–13.

730 Sullivan, M.J., Petty, N.K., Beatson, S.A., 2011. Easyfig: A genome comparison visualizer.
731 Bioinformatics 27, 1009–1010.

732 Tang, C.J., Zheng, P., Ding, S., Lu, H.F., 2014. Enhanced nitrogen removal from ammonium-rich
733 wastewater containing high organic contents by coupling with novel high-rate ANAMMOX
734 granules addition. Chem. Eng. J. 240, 454–461.

735 Tang, X., Guo, Y., Jiang, B., Liu, S., 2018a. Metagenomic approaches to understanding bacterial
736 communication during the anammox reactor start-up. Water Res. 136, 95–103.

737 Tang, X., Guo, Y., Wu, S., Chen, L., Tao, H., Liu, S., 2018b. Metabolomics uncovers the regulatory
738 pathway of acyl-homoserine lactones based quorum sensing in anammox consortia. Environ. Sci.
739 Technol. 52, 2206–2216.

740 Van de Graaf, A.A., Mulder, A., De Bruijn, P., Jetten, M.S.M., Robertson, L.A., Kuenen, J.G., 1995.
741 Anaerobic oxidation of ammoinium is a biologically mediated process. Appl. Environ. Microbiol.
742 61, 1246–1251.

743 Van De Vossenberg, J., Rattray, J.E., Geerts, W., Kartal, B., Van Niftrik, L., Van Donselaar, E.G.,

744 Sinninghe Damsté, J.S., Strous, M., Jetten, M.S.M., 2008. Enrichment and characterization of
745 marine anammox bacteria associated with global nitrogen gas production. Environ. Microbiol. 10,
746 3120–3129.

747 Van de Vossenberg, J., Woebken, D., Maalcke, W.J., Wessels, H.J.C.T., Dutilh, B.E., Kartal, B.,
748 Janssen-Megens, E.M., Roeselers, G., Yan, J., Speth, D., Gloerich, J., Geerts, W., Van der Biezen,
749 E., Pluk, W., Francoijs, K.J., Russ, L., Lam, P., Malfatti, S.A., Tringe, S.G., Haaijer, S.C.M., Op
750 den Camp, H.J.M., Stunnenberg, H.G., Amann, R., Kuypers, M.M.M., Jetten, M.S.M., 2013. The
751 metagenome of the marine anammox bacterium "Candidatus Scalindua profunda" illustrates the
752 versatility of this globally important nitrogen cycle bacterium. Environ. Microbiol. 15,
753 1275–1289.

754 Wagner, G.P., Kin, K., Lynch, V.J., 2012. Measurement of mRNA abundance using RNA-seq data:
755 RPKM measure is inconsistent among samples. Theory Biosci. 131, 281–285.

756 Wang, Y., Ma, X., Zhou, S., Lin, X., Ma, B., Park, H.D., Yan, Y., 2016. Expression of the nirS, hzsA,
757 and hdh genes in response to nitrite shock and recovery in Candidatus Kuenenia stuttgartiensis.
758 Environ. Sci. Technol. 50, 6940–6947.

759 Wolfe, A.J., 2005. The acetate switch. Microbiol. Mol. Biol. Rev. 69, 12–50.

760 Wu, S., Bhattacharjee, A.S., Dulith, B.E., Goel, R., 2016. Whole community metatranscriptomics to
761 study dynamics of functional genes in partial nitritation - anammox systems under low
762 temperatures. Proc. Water Environ. Fed. 2016, 1992–2007.

763 Zengler, K., Zaramela, L.S., 2018. The social network of microorganisms - How auxotrophies shape
764 complex communities. Nat. Rev. Microbiol. 16, 383–390.

765 Zhao, Y., Liu, S., Jiang, B., Feng, Y., Zhu, T., Tao, H., Tang, X., Liu, S., 2018. Genome-centered
766 metagenomics analysis reveals the symbiotic organisms possessing ability to cross-feed with
767 anammox bacteria in anammox consortia. Environ. Sci. Technol. 52, 11285–11296.

Table and figures

Table 1 Genome statistics of 14 draft metagenome-assembled genomes recovered from the anammox community.

Bin ID	Taxonomy	Completeness (%)	Contamination (%)	Genome size (bp)	Number of scaffolds	N50 length	GC (%)	Predicted genes
AMX1	Bacteria; Planctomycetes; Planctomycetia; Planctomycetales; Planctomycetaceae; *Jettenia*	93	3	3,667,307	88	64,658	40.0	3,120
AMX2	Bacteria; Planctomycetes; Planctomycetia; Planctomycetales; Planctomycetaceae; *Brocadia*	98	2	3,912,452	92	73,161	42.3	3,488
PLA1	Bacteria; Planctomycetes	94	7	4,191,635	132	55,477	63.5	3,592
PLA2	Bacteria; Planctomycetes	98	2	4,212,226	64	97,350	65.6	3,367
CFX1	Bacteria; Chloroflexi; Anaerolineae	98	5	10,306,408	689	28,785	55.1	9,340
CFX2	Bacteria; Chloroflexi	89	3	3,596,698	250	24,529	56.9	3,451

CFX3	Bacteria; Chloroflexi; Anaerolineae	94	1	3,418,579	52	106,613	60.2	3,228
CFX4	Bacteria; Chloroflexi	97	5	4,405,196	173	48,484	56.5	4,195
CFX5	Bacteria; Chloroflexi	99	2	5,283,747	22	384,718	51.2	4,504
PRO1	Bacteria; Proteobacteria; Betaproteobacteria	95	1	3,183,021	96	79,901	66.5	3,346
PRO2	Bacteria; Proteobacteria; Alphaproteobacteria	78	3	2,465,431	337	9,252	66.3	2,696
PRO3	Bacteria; Proteobacteria; Gammaproteobacteria	84	1	2,290,772	67	42,710	68.3	2,187
CYA1	Bacteria; Cyanobacteria	79	0	2,542,560	13	241,538	68.7	2,184
CPR1	Bacteria; unclassified bacteria	74	1	796,921	115	9,410	44.3	887

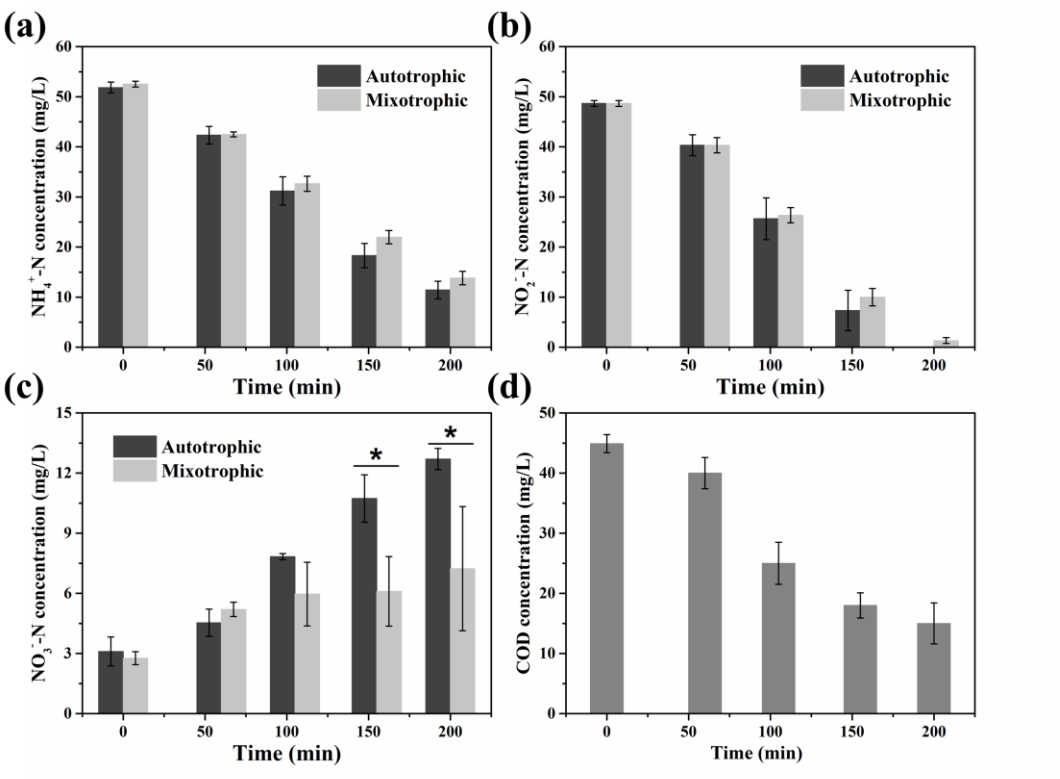

770

771 **Figure 1** Concentrations of (a) NH_4^+-N, (b) NO_2^--N, (c) NO_3^--N in autotrophic and

772 mixotrophic groups in batch tests, and (d) concentration of COD in mixotrophic group.

773 Error bars are defined as s.e.m. (n = 3, biological replicates). * represents $p < 0.05$ by

774 two-tail t-test.

775

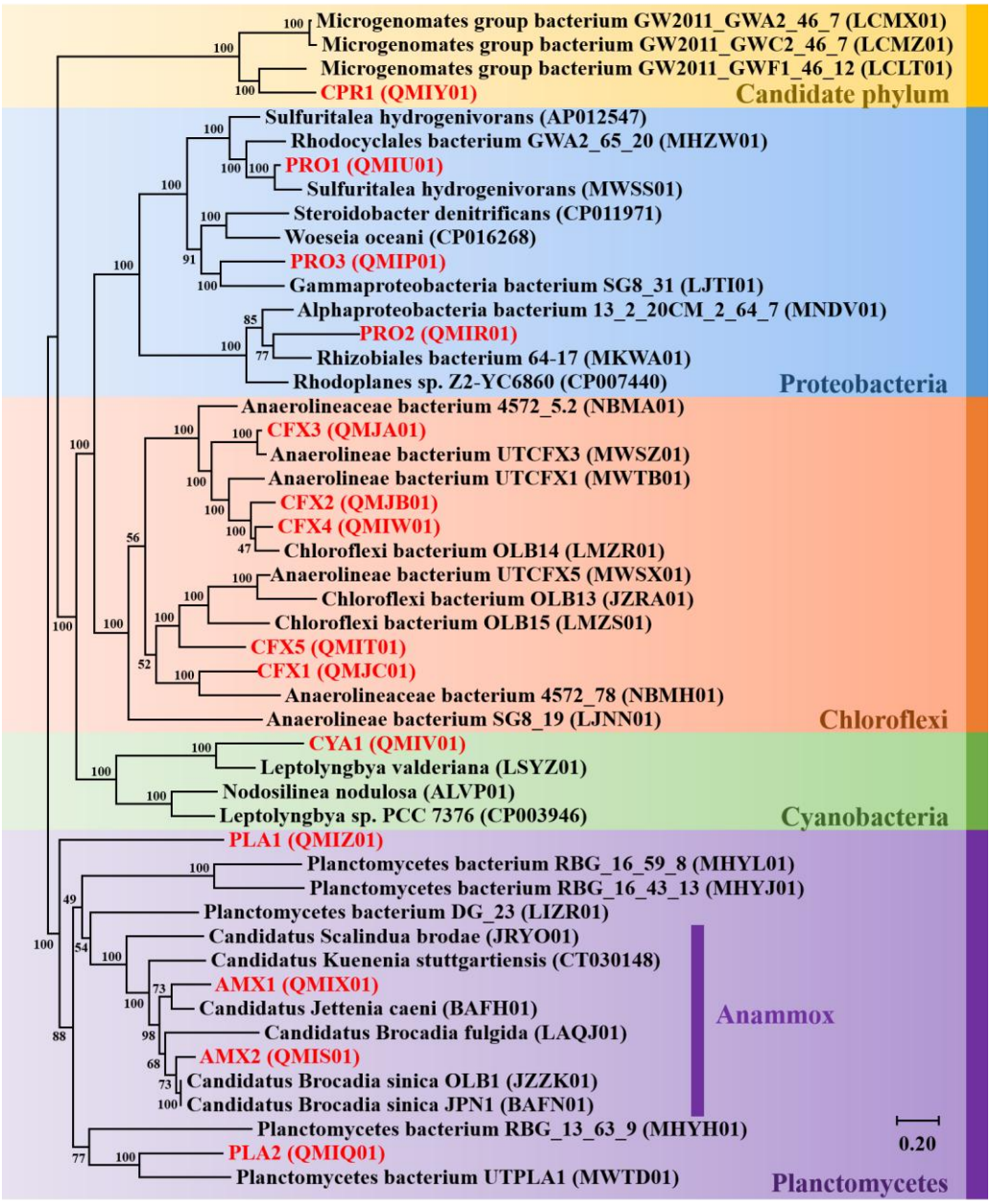

Figure 2 Phylogenetic tree of all recovered draft genomes from the anammox consortia. Draft metagenome-assembled genomes recovered from this study are shown in red, and closely related genomes downloaded from the NCBI are shown in black. GenBank accession numbers of each genome are also presented. Bootstrap support values are represented at branch nodes.

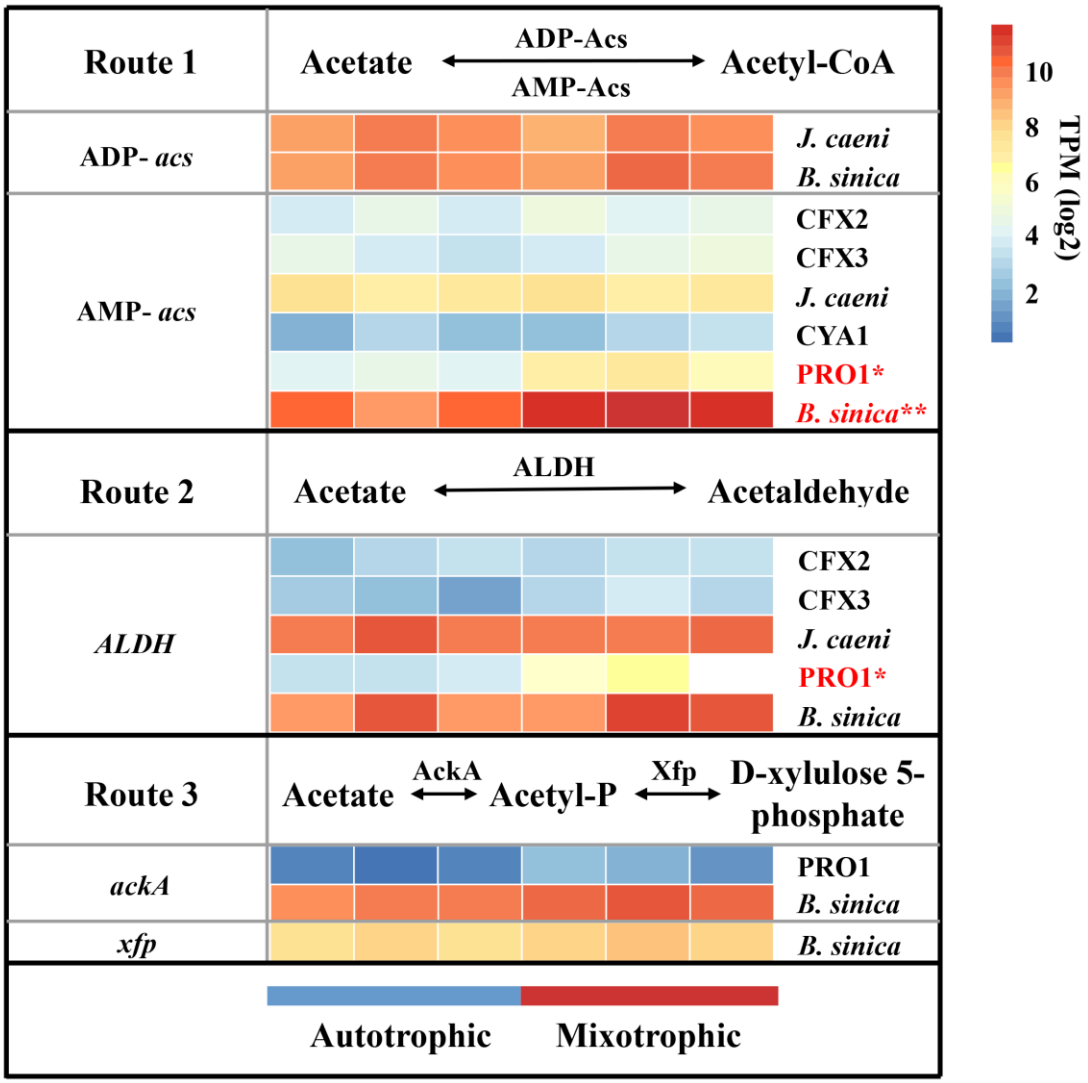

783

784 **Figure 3** Three main acetate metabolic pathways in anammox consortia. Heatmap

785 exhibits gene expression profiles (Z score) in autotrophic and mixotrophic. Red

786 indicates significant difference ($p < 0.05$ by two-tail t-test). *: $p < 0.05$; **: $p < 0.01$.

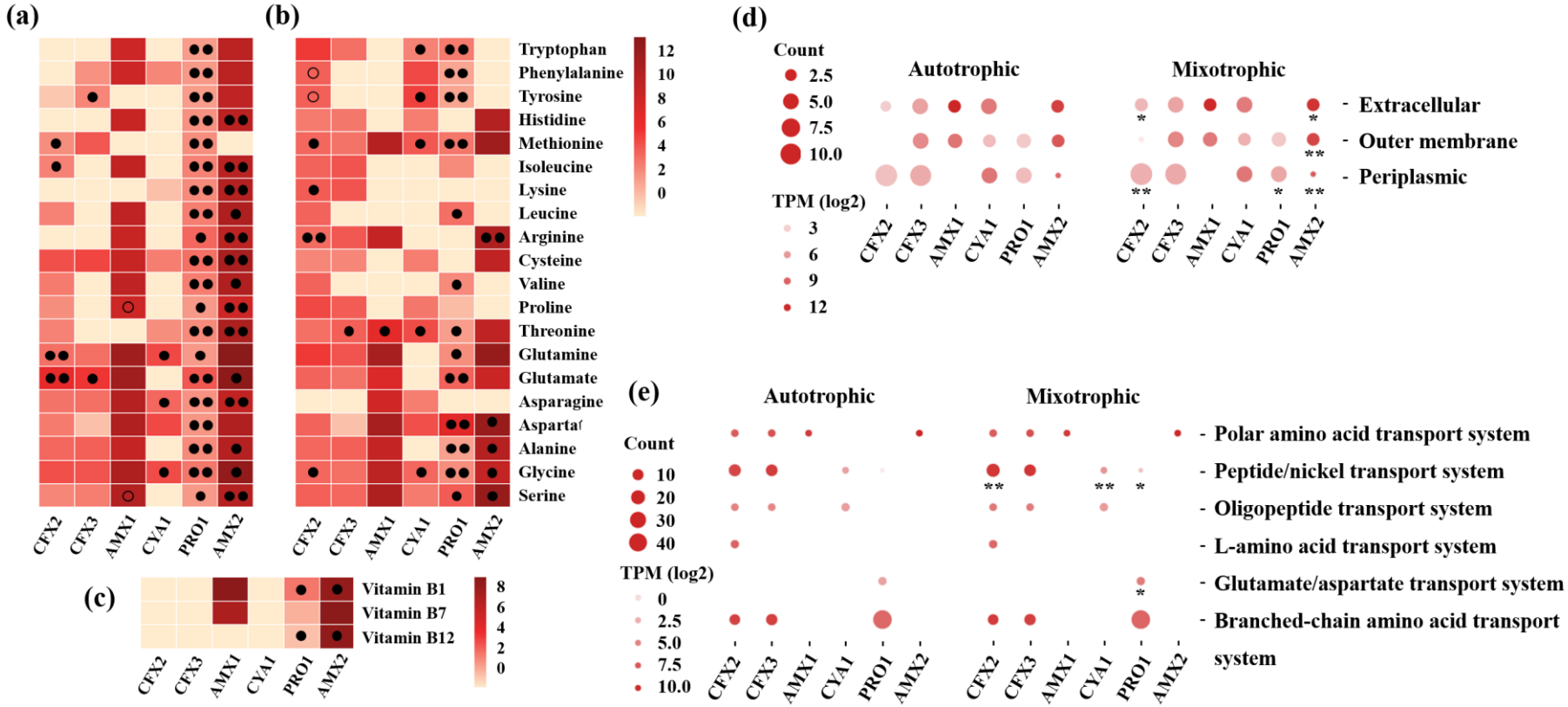

Figure 4 Expression profile of genes involved in amino acids and B-vitamins cross-feedings in anammox consortia. Relative gene expression of (a) amino acid biosynthetic pathways, (b) amino acid degradation pathways and (c) vitamin B biosynthetic pathways in each species. Color

intensity represents log2 transformed gene expression level, which was obtained by median TPM values across each pathway. One black dot represents $p < 0.05$ by t-test, and two dots represents $p < 0.01$ by t-test. (d) Peptidases possibly involved in extracellular protein degradation of each species in autotrophic and mixotrophic anammox consortia. The location of peptidase was predicted using the subcellular localization predictor (CELLO). (e) Amino acid and oligopeptide transporters of each species in autotrophic and mixotrophic anammox consortia. Count number was represented by bubble diameter, and gene expression was represented by bubble colour intensity. * represents $p < 0.05$ by two-tail t-test, ** represents $p < 0.01$ by two-tail t-test. AMX1 and AMX2 represents *J. caeni* and *B. sinica*, respectively.

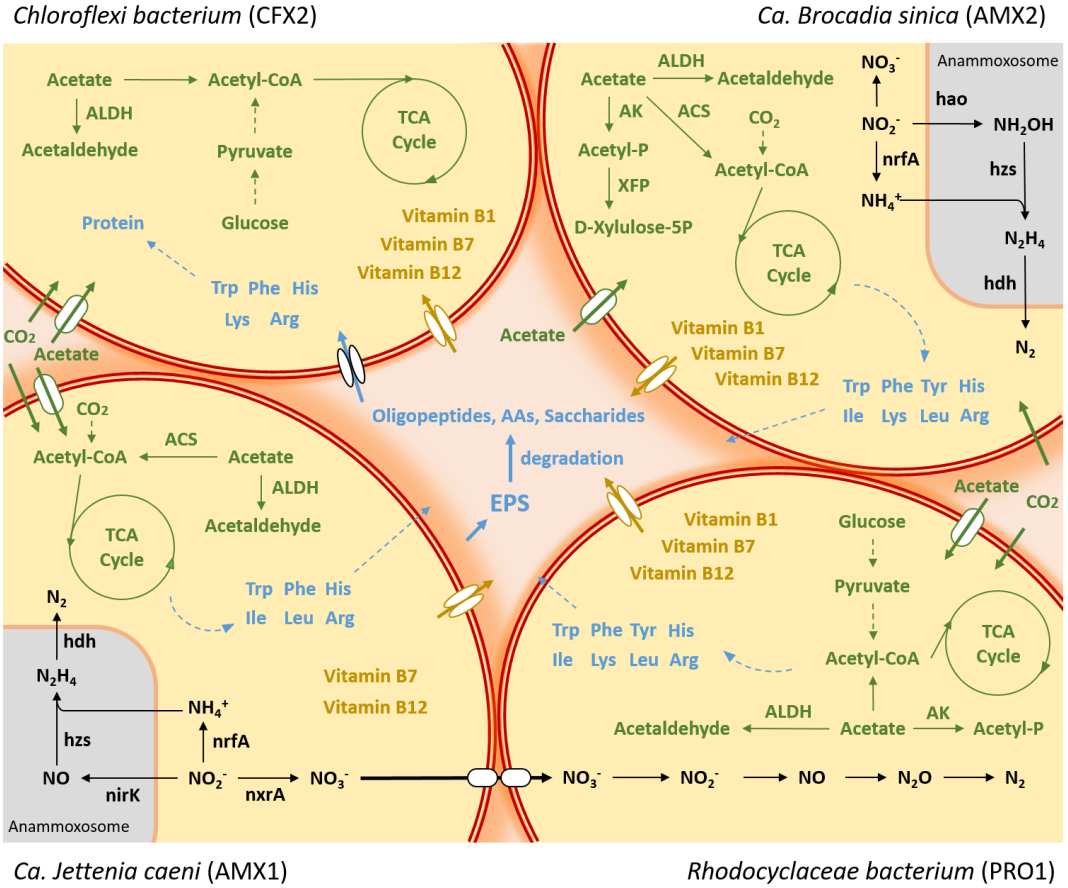

796

797 **Figure 5** Proposed metabolic interactions among *J. caeni*, *B. sinica*, *Chloroflexi*

798 *bacterium* (CFX2) and *Rhodocyclaceae bacterium* (PRO1) in anammox consortia.